

# The Alhama de Murcia fault (SE Spain), a seismogenic fault in a diffuse plate boundary: Seismotectonic implications for the Ibero-Magrebian region

E. Masana

Departament de Geodinàmica i Geofísica, Universitat de Barcelona, Barcelona, Spain

J. J. Martínez-Díaz and J. L. Hernández-Enrile

Departamento de Geodinámica, Facultad de Ciencias Geológicas, Universidad Complutense, Madrid, Spain

P. Santanach

Departament de Geodinàmica i Geofísica, Universitat de Barcelona, Barcelona, Spain

Received 20 December 2002; revised 15 September 2003; accepted 26 September 2003; published 2 January 2004.

[1] The shortening between the African and the Iberian plates is absorbed by a number of faults distributed over a very wide zone with very low slip rates and long periods of seismic loading. Thus a seismotectonic map based only on faults associated with seismicity or with expressive geomorphic features is incomplete. It is possible to characterize seismogenic faults using paleoseismology. First, paleoseismological results based on trenching analysis in the eastern Betics (Lorca-Totana segment of the Alhama de Murcia fault) are presented. The main paleoseismic parameters of this fault segment are (1) a minimum of two to three  $M_w$  6.5–7 earthquakes in the last 27 kyr (shortly before 1650 A.D., between 830 and 2130 B.C. and shortly before 16.7 ka, respectively), with a mean recurrence period of 14 kyr, and a very short elapsed time, and (2) a net slip rate of 0.07–0.6 mm/yr during the last 30 kyr. These results were extrapolated to the rest of the known active faults in the eastern Betics and were added to the slip rates of the active faults at the African margin. The total slip rate of the transect, which crosses de Alhama de Murcia fault in Spain and reaches the Cheliff basin (Algeria), would represent 21–82% of the total shortening between Africa and Eurasia estimated from plate motion models and seismic moment summation. A number of factors could account for this discrepancy: (1) hidden seismogenic faults in the emerged areas, (2) absence of correlation between current and late Pleistocene slip rates, (3) extensive small faults that are undetected and that absorb a significant amount of the deformation, and (4) possible overestimation of the convergence rates. **INDEX TERMS:** 7221 Seismology: Paleoseismology; 7230 Seismology: Seismicity and seismotectonics; 7215 Seismology: Earthquake parameters; 8150 Tectonophysics: Plate boundary—general (3040); **KEYWORDS:** eastern Betics, Alhama de Murcia fault, paleoseismology, trenching, seismotectonics, plate boundary

**Citation:** Masana, E., J. J. Martínez-Díaz, J. L. Hernández-Enrile, and P. Santanach (2004), The Alhama de Murcia fault (SE Spain), a seismogenic fault in a diffuse plate boundary: Seismotectonic implications for the Ibero-Magrebian region, *J. Geophys. Res.*, *109*, B01301, doi:10.1029/2002JB002359.

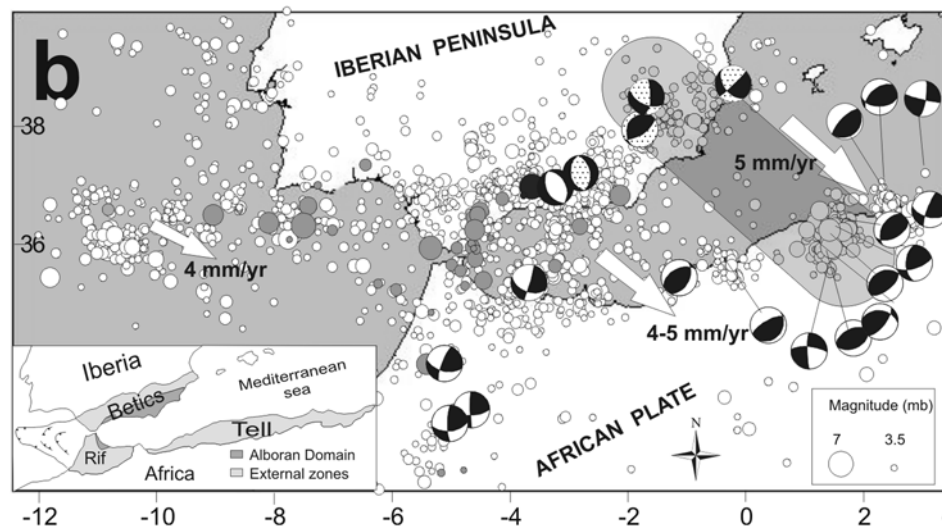
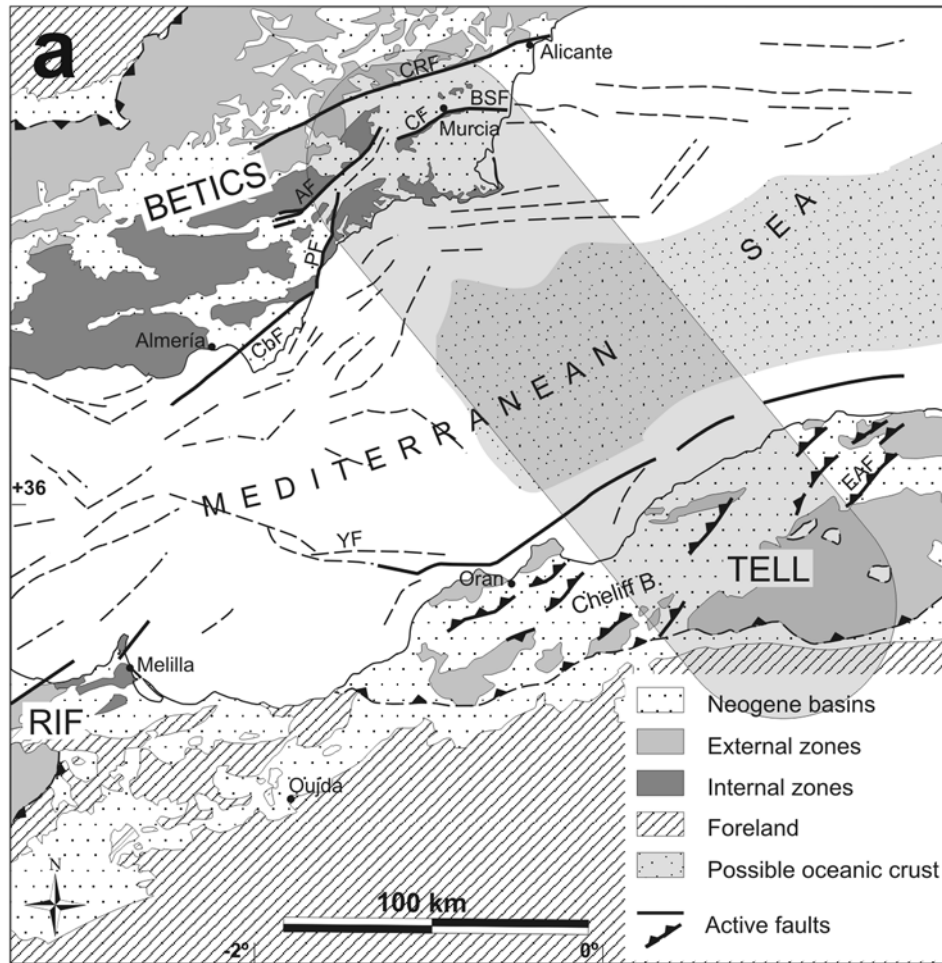
## 1. Introduction

[2] Iberia and Africa converge at a very slow rate, 4.5–5.6 mm/yr [Argus *et al.*, 1989; DeMets *et al.*, 1990, 1994; Kiratzi and Papazachos, 1995; McClusky *et al.*, 2003; Pondrelli, 1999] through a diffuse collisional plate boundary. The width of this boundary has been defined by its seismicity and recent deformation [McKenzie, 1972; López *et al.*, 1987; Buforn *et al.*, 1995; López *et al.*, 1995; Sanz de Galdeano *et al.*, 1995; Meghraoui *et al.*, 1996]. The area

under deformation is 1500 km wide in some parts and includes the Betics, the Pyrenees, the Rif-Tell, and the Atlas Mountains with the Alboran sea between the Betics and the Rif-Tell (Figure 1). The slow convergence rate and the diffuse boundary suggest the partition of the shortening across the boundary zone between a number of structures with slow slip rates, which do not facilitate clear evidence of their tectonic activity. Although large earthquakes enable the detection of some of these active faults, many remain hidden because of the long recurrence periods of their maximum earthquakes. It is possible that the largest earthquakes of some seismogenic faults may not have been historically recorded.

[3] Slow moving active faults are often difficult to identify despite their seismogenic nature [D'Addezio et al., 1995; Pantosti et al., 1996; Crone et al., 1997; Masana et al., 2001; Martínez-Díaz et al., 2001]. Paleoseismology can provide evidence of seismogenic activity along silent faults and can characterize this activity in terms of slip rate and amount of deformation absorbed by individual faults. Although a number of studies have revealed recent tectonic activity along some of the faults, few analyses focus on their seismogenic

behavior. Paleoseismic data of the El Asnam earthquake zone (Algeria) provide some constraints for the active and seismic tectonics in the African plate [Aoudia and Meghraoui, 1995; Meghraoui and Doumaz, 1996; Morel and Meghraoui, 1996]. By contrast, the seismogenic behavior of faults in the Iberian plate has been neglected to date. Southeast of the Pyrenees, Masana [1996] and Masana et al. [2001] provide evidence of seismogenic activity along the El Camp normal fault, several hundred kilometers north of the collisional



zone. In the Betics, south of the Granada basin, *Reicherter* [2001] relates the 1885 earthquake to the normal fault at Ventas de Zafarraya using a paleoseismological approach, and *Alfaro et al.* [2001] describe the recent tectonics of the El Padul normal fault without dating and characterizing the individual earthquakes.

[4] The main aim of this paper is the paleoseismological characterization of the Lorca-Totana segment of the Alhama de Murcia fault, which is one of the most active faults in the eastern Betics. The parameters obtained are extrapolated to the rest of the known active faults of a transect parallel to the Eurasia-Africa convergence vector to obtain an approximate value of the shortening absorbed by the known active faults along this transect. The transect crosses de Alhama de Murcia fault in Spain and reaches the Cheliff basin in Algeria. A comparison of this total shortening rate estimated from the paleoseismological data to the convergence rate of the Iberian and African plates along the considered transect shows discrepancies, raising a discussion about the seismotectonic model across the diffuse Iberian-African plate boundary.

## 2. The Betics in the Ibero-Maghrebian Region

[5] The Betics and the Rif, the westernmost Alpine ranges, are linked by the Gibraltar arc at the boundary between the African and Iberian plates. From west to east, this plate boundary extends from the Azores to the Straits of Gibraltar and continues through the south of the Iberian Peninsula, the Alboran Sea, and northern Morocco, Algeria and Tunisia (Figure 1). Along the westernmost part of this boundary the plates are currently formed by oceanic lithosphere whereas, from Gibraltar to Tunisia, the two colliding plates are composed of continental lithosphere. The Alboran Sea, which separates both ranges, is formed by an extremely thinned continental lithosphere and oceanic crust to the east [*Comas et al.*, 1999].

[6] The Betics and the Rif show an apparently symmetrical structure. They are both made up of internal units (Alpujarride, Malaguide and Nevadofilabride in the Betics, and Sebides and Ghomarides in the Rif), external zones (foreland basins), and several Neogene to Quaternary basins superimposed onto the previous structure and limited by E-W and NE-SW faults. The different opening velocities along the north and south Mid-Atlantic Ridge have transformed the Eurasian-African plate boundary into a transform fault since Triassic times. The African and Iberian passive margins formed and the Ligurian Ocean opened in the Jurassic and early Cretaceous [*Sanz de Galdeano*, 1990]. The Late Cretaceous subduction of the oceanic

lithosphere ended and the continental collision and thickening of the crust began in the Eocene-Oligocene with the emplacement and shortening of the internal zones. During the Miocene, shortening in the external zones was coeval with the formation of the Alboran Sea under extension. Two hypotheses could account for this: (1) a roll-back, N-S, short subduction zone that migrated westward and ended in Tortonian times when the African margin reached the subduction zone (this would explain the arcuate distribution of the volcanism with the calc-alkaline rocks in the center and the rest following the Gibraltar arc [*Loneragan and White*, 1997]), and (2) a radial collapse that followed the thickening of the lithosphere due to a convective removal of the lithospheric root [*Dewey et al.*, 1989; *Platt and Vissers*, 1989; *Doblas and Oyarzun*, 1989]. During the Miocene, the Betics were, first, under a WNW-ESE maximum horizontal stress, which caused the Alpujarras and Crevillente fault systems to behave as dextral faults [*Sanz de Galdeano*, 1983, 1990]. The compressional axis rotated to a NNW-SSE direction during the Tortonian and several NE-SW (i.e., Alhama de Murcia fault) and N90°–110°E faults moved with sinistral and dextral components, respectively [*Montenat et al.*, 1987]. The same maximum horizontal stress direction has been maintained until the present with small variations [*Martínez-Díaz*, 2002]. According to seismic slip vector studies the Iberian plate is currently converging toward the African plate following an average NW-SE direction with a velocity of 5.4–5.6 mm/yr, whereas very recent results of plate motion by GPS measurements suggest 4.5 mm/yr of convergence velocity [*Argus et al.*, 1989; *DeMets et al.*, 1990, 1994; *Kiratzi and Papazachos*, 1995; *McClusky et al.*, 2003; *Pondrelli*, 1999].

[7] Although not as well constrained as along the Azores fault plane, the seismicity from 12°W to Gibraltar and along the Algerian coast is concentrated along a narrow band. By contrast, in Spain and Morocco, the seismicity is distributed over a wide zone, from the Pyrenees to the Saharan Atlas, and is mainly concentrated in the Internal zones of the Betic and Rif ranges (Figure 1). The instrumental seismicity of the 1965–1999 period [*Instituto Geográfico Nacional (IGN)*, 2001] is characterized by a continuous activity of moderate to low magnitude ( $M < 5$ ) earthquakes and by two large events, the El Asnam (Algeria,  $m_b = 6.5$ , 1980) and the Cape San Vicente (Portugal,  $m_b = 7.3$ , 1969) earthquakes [*Bufo et al.*, 1995]. The historical catalogue (Table 1) shows other catastrophic earthquakes in the area such as the Lisbon (Portugal, 1755, MSKI = X) or the Arenas del Rey (Spain, MSKI = X, 1884) earthquakes among others. Most of the seismicity is superficial (Figure 1) although in certain zones intermediate earthquakes (40–180 km deep), and a

**Figure 1.** (a) Geological map of the eastern Ibero-Maghrebian region. Oval and shaded area indicates the section across the Alhama de Murcia fault parallel to the plate boundary shortening vector. CRF, Crevillente fault; AF, Alhama de Murcia fault; CF, Carrascoy fault; BSF, Bajo Segura fault; PF, Palomares fault; CaF, Carboneras fault; YF, Yussuf fault; EAF, El Asnam rupture. Dashed lines correspond to possible recent faults in the offshore zone. (b) Seismicity of the Ibero-Maghrebian region. Epicenters deeper than 500 km are in black (only one point is visible at this scale although it corresponds to four epicenters in the same position), those between 90 and 200 km in depth are in dark gray, and those shallower than 90 km are in white. Seismicity with magnitude  $M_s > 3.5$  (data from Instituto Geográfico Nacional, 1965–1999). CMT focal mechanisms of earthquakes with  $M_s > 4.0$  since 1980 are shown: Harvard catalogue in white and Instituto Andaluz de Geofísica with dots (Harvard CMT Project, available at <http://www.seismology.harvard.edu/projects/CMT/>, and *Stich et al.* [2003]). Convergence slip vectors are from *Argus et al.* [1989] (see text for discussion).

**Table 1.** Earthquakes With Intensities >VIII and/or  $m_b$  5 in the Area Ranging Between Longitude  $-12^\circ$  to  $+4^\circ$  and Latitude  $+32^\circ$  to  $+40^\circ$ <sup>a</sup>

Locality	Year	Longitude	Latitude	Magnitude $m_b$	Intensity MSK
Atlantic Ocean	9 Dec. 1320	-10.67	36		X
Tabernes (SP)	18 Dec. 1396	-0.25	39.167		IX
Atarfe (SP)	24 April 1431	-3.6	37.2		IX
Carmona (SP)	5 April 1504	-5.6	37.4		IX
Vera (SP)	9 Nov. 1518	-1.87	37.217		IX
Almeria (SP)	22 Sept. 1522	-2.5	36.917		IX
Vilafranca (SP)	26 Jan. 1531	-9	38.95		IX-X
Fez (MOR)	23 May 1623	-5.33	34		IX
Alcoy (SP)	1645	-0.45	38.7		IX
Alhaurin (SP)	9 Oct. 1680	-4.67	36.683		IX
Argel (AL)	3 Feb. 1716	3.1	36.7		X
Enguera (SP)	23 March 1748	-0.65	39		IX
Atlantic Ocean	1 Nov. 1755	-10	37		X
Atlantic Ocean	31 March 1761	-10	37		IX
Oran (AL)	9 Oct. 1790	-0.6	35.7		IX-X
Dalias (SP)	25 Aug. 1804	-2.8	36.8		IX
Atlantic Ocean	2 Feb. 1816	-10	35		IX
Mascara (AL)	March 1819	0.1	35.4		IX
Blida (AL)	2 March 1825	2.9	36.5		X-XI
Torrevecija (SP)	21 March 1829	-0.7	38.1		X
Mediterranean	9 Feb. 1850	4	36.7		IX
Blida (AL)	9 March 1858	2.9	36.5		IX
Setubal (POR)	11 Nov. 1858	-9	38.2		IX
Blida (AL)	2 Jan. 1867	2.83	36.467		X-XI
Arenas (SP)	25 Dec. 1884	-3.98	36.95		X
El Asnam (AL)	29 Nov. 1887	0.33	35.583		IX-X
Dupleix (AL)	15 Jan. 1891	1.8	36.5		X
Romara (MOR)	21 Jan. 1909	-5.6	35.5		IX
Benavente (POR)	23 April 1909	-8.82	38.95		IX
Masqueray (AL)	24 June 1910	3.42	36.05	6.4	X
Atlantic Ocean	11 July 1915	-11.8	35.5	6.2	V
Fromentin (AL)	19 Nov. 1922	1.08	36.283	5.6	IX
Cavaignac (AL)	25 Aug. 1922	1.2	36.417	5.1	IX-X
Ben Chavane (AL)	5 Nov. 1924	2.9	36.65	5.2	IX
Carnot (AL)	7 Sept. 1934	1.72	36.233	5.0	IX
Bousemrah (MOR)	13 March 1948	0.1	33	5.0	IX
El Asnam (AL)	9 Sept. 1954	1.5	36	6.0	IX
El Asnam (AL)	9 Sept. 1954	1.5	36	6.7	X-XI
El Asnam (AL)	9 Sept. 1954	1.47	36.283	6.7	X-XI
Tenes (AL)	10 Sept. 1954	1.3	36.6	6.0	VIII
Fodda (AL)	12 Oct. 1954	1.7	36.25	6.0	VII
Bou Medfa (AL)	7 Nov. 1959	2.5	36.4	5.1	IX
Cadiz Gulf	15 March 1964	-7.75	36.131	6.2	VII
Atlantic Ocean	28 Feb. 1969	-10.813	35.985	7.3	VII
El Asnam (AL)	10 Oct. 1980	1.45	36.153	6.5	IX
Les Attafs (AL)	10 Oct. 1980	1.648	36.166	6.2	

<sup>a</sup>Catalogue of the Instituto Geografico Nacional (Spain) and of the European Mediterranean Seismological Center. POR, Portugal; AL, Algeria; MOR, Morocco; SP, Spain.

far deeper hypocenters (over 600 km) have also been recorded [Buforn *et al.*, 1991, 1995]. The intermediate seismicity is possibly linked to an ancient subduction zone or to delamination [Buforn *et al.*, 1995] and the few deep earthquakes could be attributed to a broken old subducted slab [Udias *et al.*, 1976; Cung and Kanamori, 1976; Grimison and Cheng, 1986].

[8] The epicentral map suggests few bands of earthquakes. A number of epicenters are located along the deformation zone controlled by the Alhama de Murcia, Carboneras, and Palomares faults in the Betics, and with lower intensity, along the Agadir-Nekor seismic belt in the Middle Atlas.

### 3. The Alhama de Murcia Fault

[9] The Alhama de Murcia fault (AMF), first described as a strike-slip fault by Bousquet and Montenat [1974], is

located in the eastern Betics and runs along 100 km from the Huercal-Overa depression to the surroundings of Murcia (Figure 1). According to geophysical data (gravimetry and vertical electric sounding) it could reach the Crevillente fault to the north [Gauyau *et al.*, 1977]. This NE-SW trending fault (Figure 2) bounds the Guadalentin Neogene depression to the northwest. The late Miocene left-lateral and reverse oblique-slip probably controlled the evolution of the Lorca and Alhama-Fortuna Neogene basins under a NNW-SSE to NNE-SSW compression field [Bousquet and Montenat, 1974; Bousquet *et al.*, 1978; Bousquet, 1979; Armijo, 1977; Martínez-Díaz and Hernández-Enrile, 1992a, 1992b]. Recent neotectonic studies [Martínez-Díaz and Hernández Enrile, 1992b, 1996, 1999; Baena *et al.*, 1993; Silva *et al.*, 1993] confirm the Quaternary stress field.

[10] On the basis of their geometry, fractal signature, and seismicity, Silva *et al.* [1992] proposed the subdivision of

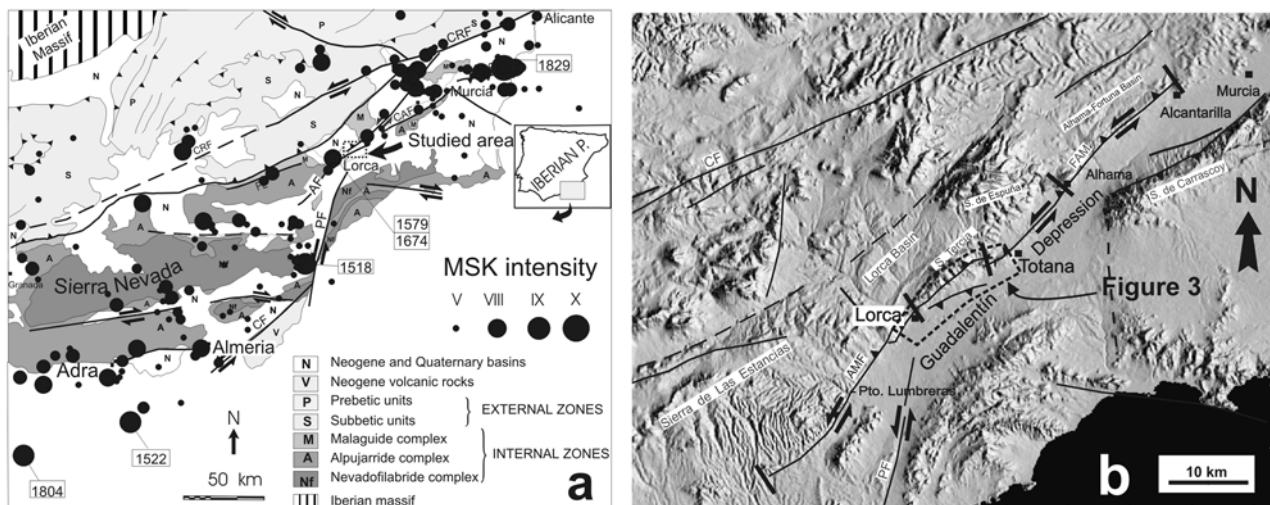


**Figure 2.** (a) Macroseismicity map of eastern Betics with the main Neogene faults. Indicated fault movements correspond to late Neogene. CRF, Crevillente fault; AF, Alhama de Murcia fault; CF, Carrascoy fault; PF, Palomares fault; CF, Carboneras fault. (b) Topographical model of the surroundings of the Alhama de Murcia fault, next to the Neogene Guadaleñín depression. The segment boundaries along the Alhama de Murcia fault are indicated by black bars.

the fault into four segments: Huerca Overa-Lorca (NNE-SSW), Lorca-Alhama (NE-SW), Alhama-Alcantarilla (NNE-SSW), from Alcantarilla to the north. This proposition has been modified by *Martínez-Díaz and Hernández Enrile* [1999], who supplied information concerning the recent tectonic history of the fault, and the morphologic features of the ranges bounded by the fault (Figure 2b). They suggest a subdivision of the Lorca-Alhama part into two segments and do not consider the fault to the north of Alcantarilla. The result is four segments along the whole fault from south to north: (1) Puerto Lumbreras (or Huerca Overa)-Lorca (37 km), with a horse tail termination to Huerca Overa, moderate concentration of epicenters and the evident relief of the Las Estancias range, (2) Lorca-Totana (16 km) where the fault controlled the evolution of the Neogene Lorca basin, currently bounding the La Tercia range and with the maximum concentration of seismicity, (3) Totana-Alhama de Murcia (17 km), and (4) Alhama de Murcia-Alcantarilla (23 km) which controlled the evolution of a depression to the NW but shows low geomorphologic fault expression. The different seismogenic behavior of these segments has not been proved and consequently the rupture of the whole fault cannot be ruled out. Our paleoseismic study focused attention on the Lorca-Totana segment (Figure 2), where Quaternary sediments are trapped by the recent activity of the fault (Figure 3).

#### 4. Seismogenic Characterization of the Lorca-Totana Segment

[11] The Lorca-Totana segment of the Alhama de Murcia fault is a 16-km-long structure composed of two main NE-SW fault branches: (1) a northwestern reverse fault strongly dipping to the northwest and bounding the La Tercia range to the SE and (2) a southeastern left-lateral and high-angle reverse fault dipping to the southeast with oblique slip. The northwestern fault separates the Malaguide and Alpujarride

units which make up the La Tercia range from the Quaternary sediments deposited to the southeast in a NE-SW elongated depression. The southeastern fault separates the Quaternary sediments to the northwest (the elongated basin) from the Miocene sediments to the southeast. The combined activity of the two faults is responsible for the formation of the NE-SW elongated Quaternary basin, which could behave as a damming corridor for the sediments coming from the La Tercia range. Both strands join together near the town of Lorca to the southwest whereas the southeastern fault strand vanishes to the northeast near Totana.

[12] The historical seismic catalogue (Table 2) contains references of a number of MSK  $I > VI$  earthquakes linked to the Alhama de Murcia fault, three with MSK  $I = VIII$  [*Martínez Solares and Mezcua*, 2002]. Of these, the earthquakes of Lorca 1579, 1674, and 1818; Murcia 1743; Totana 1907; Lorquí 1911; and Fortuna 1944 stand out. Most of the seismicity is concentrated along the central part of the fault (mainly along the Lorca-Totana segment), and no historical seismicity has been recorded in the southern segment (Puerto Lumbreras-Lorca). In the Lorca-Totana segment the largest earthquakes occurred in 1579 (MSK  $I = VII$ ) and 1674 (MSK  $I = VIII$ ) [*Martínez Solares and Mezcua*, 2002] with epicenter in Lorca. The most latter was a series of at least three earthquakes, two of them of MSK  $I = VII$  and the strongest one of  $I = VIII$ . The reports of another earthquake in Lorca (1818, MSK  $I = VII$ ), describe how the landscape was modified by the earthquake “hundimiento de unas tierras entre Lorca y Totana” collapse of some parts of the land between Lorca and Totana [*Martínez-Guevara*, 1984], which could be interpreted as landslides. A correlation between MSK  $I = VIII$  and a  $m_b = 6.0$  has been obtained from the earthquake population analysis in the area [*Martínez-Díaz*, 1998]. The instrumental seismicity, which never exceeds 4.5, is mainly concentrated along the southeastern Lorca-Totana fault and is also sporadic in the Guadaleñín depression [*Amores et al.*, 2002]. The hypo-

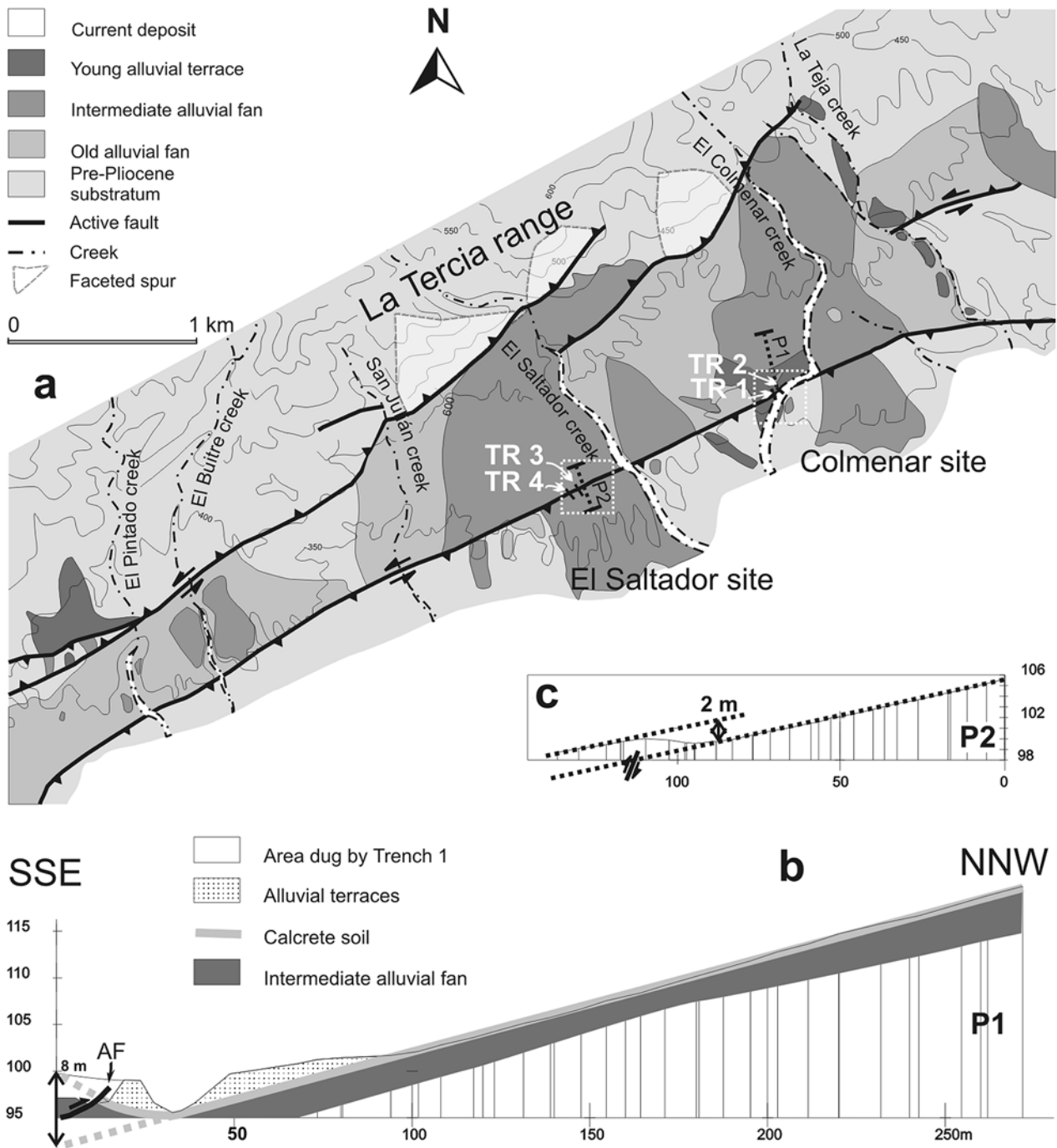


**Figure 3.** (a) Geomorphological sketch of the studied area between Lorca and Totana. Microtopographic profiles and trenches 1 to 4 are located on the map. (b) Microtopographic profile along the El Saltador fan and across the fault. (c) Geological cross section of the Colmenar site based on a microtopographical profile. Note that the offset of the calcrete soil on top of the intermediate alluvial fan is 8 m.

centers are shallow, mostly located around 10 km depth [Martínez-Díaz, 1998].

[13] A geomorphological analysis revealed three depositional units filling the upper part of the depressed corridor (Old alluvial fan, Intermediate alluvial fan, and Young alluvial terrace) (Figure 3). These recent units are deposited over late Miocene rocks (upper Tortonian yellow marls and

laminated Messinian gypsum [Montenat et al., 1987]. The Old alluvial fan unit is composed of alluvial gravels, sands and clays, displaying highly developed calcrete soils. The Intermediate alluvial fan unit shows a similar composition with a reddish color and moderately developed calcrete soils on top. Finally, the Young alluvial terraces are gray in color, made up of gravels, sands and, locally, light clays, and

**Table 2.** Historical Seismicity Along the Alhama de Murcia Fault<sup>a</sup>

Longitude	Latitude	Date	Time, LT	Io (MSK)	Locality
-1.700	37.699	30 Jan. 1579	-	VII	Lorca
-1.700	37.699	10 Aug. 1674	-	VI	Lorca
-1.700	37.699	28 Aug. 1674	1000:00	VIII	Lorca
-1.700	37.699	29 Aug. 1674	-	VII	Lorca
-1.100	37.999	9 March 1743	1600:00	VII	Murcia
-1.100	37.999	15 Aug. 1746	-	VI–VII	Murcia
-1.700	37.699	20 Dec. 1818	0945:00	VII	Lorca
-1.416	37.866	11 Nov. 1855	0400:00	VI–VII	Alhama de Murcia
-1.930	37.366	10 Feb. 1863	1110:00	VI–VII	Huerca Overa
-1.250	38.083	16 Jan. 1883	0340:00	VI–VII	Ceuti
-1.500	37.799	16 April 1907	1730:00	VII	Totana
-1.216	38.016	21 March 1911	1415:35	VIII	Cotillas
-1.200	38.099	3 April 1911	1111:11	VIII	Lorqui
-1.200	38.099	10 May 1911	0955:30	VII	Lorqui
-1.200	38.099	16 May 1911	2220:21	VII	Lorqui
-1.266	38.033	28 Jan. 1917	2232:31	VII	Torres de Cotillas
-1.233	38.066	3 Sept. 1930	0959.58.0	VII	Lorqui
-1.150	38.166	23 Feb. 1944	2234:10	VII	Fortuna

<sup>a</sup>Data from López Marinas [1977a, 1977b, 1978], Martínez-Guevara [1984], and Martínez Solares and Mezcuá [2002].

contain slightly developed carbonatic soils. The lower units contain a large amount of Tortonian carbonatic pebbles whereas the upper limits have a predominance of metamorphic pebbles.

[14] A right stepping array of NE-SW kilometer-long faults, which are mainly dip-slip faults because of the faceted spurs, forms the northwestern fault. The right stepping arrangement of these faults could account for an inherited geometry and does not reflect the present fault activity given the left lateral movement of the Alhama de Murcia fault. Although Plio-Quaternary sediments (Old and Intermediate alluvial fans in Figure 3a) are deformed by this fault, no large fault scarps or deformation were found in the most recent sediments (upper Intermediate alluvial fan and Young alluvial terrace of Figure 3a). In contrast, the southeastern fault clearly deforms the young units. This suggests that current tectonic activity is taking place along the southeastern fault. This fault was therefore selected for paleoseismic study because of its prominent geomorphological expression and current tectonic indicators as recorded by the sediments following the cumulative offset.

[15] Two alluvial fans, Colmenar and El Saltador, which belong to the Intermediate alluvial fans (Figure 3a), reach the Guadalentin basin crossing the southeastern fault. Figure 3c shows 8 m of vertical offset on top of the Colmenar alluvial fan, which was deduced from the microtopographic profiling of the fan surface and the position of this same surface buried at trench 1. An additional profile to the west of trench 1 suggests 2.5 m of vertical offset. Two meters were measured along the El Saltador Intermediate alluvial fan surface (Figure 3b).

#### 4.1. Paleoseismic Studies at the Colmenar Creek Site

[16] At the intersection of the Colmenar fan with the southeastern fault, Colmenar creek, which flows from the La Tercia range toward the Guadalentin in a NW-SE direction, turns abruptly to the WSW (parallel to the fault), and recovers its NW-SE trend for several hundred meters downstream. The fault exposure generated by the river incision on the right bank was analyzed for paleoseismology (trench 2). Trench 1 was dug across the fault where the

young terraces (Holocene in age as a result of radiocarbon dating according to Martínez-Díaz *et al.* [2001]) are preserved next to the fault.

[17] Trench 1 (Figure 4) shows the deposits of the alluvial terrace (C–F) that overlies the intermediate alluvial fan (A, B), and also the Miocene yellow marls and gypsum, (O). The whole sequence of intermediate and young deposits is tilted (in different dips) to the northwest because of the reverse movement of the fault. Four highly SE dipping reverse fault zones were observed (2–5) affecting units A to B. The contact between the deformed and eroded intermediate alluvial fan generation deposits, Quaternary in age, and the Neogene marls, silts and gypsum is a vertical unconformity (number 1 in Figure 4). The faults labeled 2, 3 and 4 in Figure 4 cut the beds of this alluvial fan and show a slip larger than the trench depth, whereas the slip of fault 5 is of around one meter (see unit A<sub>1</sub> in trench 1). The kinematic behavior of the fault was only constrained by the reverse component on trench walls in the absence of slickensides on the fault planes and hence a strike-slip component was not confirmed at trench 1.

[18] Trench 2 (Figure 4) shows a highly deformed area in the lower part of the wall, produced by several SE low dipping reverse faults that converge in the southeastern lowermost part of the trench. As in trench 1, a vertical contact (unconformity) is visible between Miocene marls and Quaternary beds (number 1 in Figure 4). The faults numbered 2 to 4 show reverse slip on the trench wall. Close to the unconformity, some vertical bedding planes separating gravel from silt beds show horizontal slickensides, suggesting interbedding slip with strike-slip component, although few dip-slip slickensides are also observed.

[19] The stratigraphic units of both trenches are well correlatable and tilted in the same sense. In addition, trench 2 shows a better exposure of the very local unit C formed by red to yellowish silty layers with some sparse pebbles, tilted to the north. Unit E covers units C and D by means of an erosive contact with channel structures. Radiocarbon dating reveals that unit D is younger than unit C (Table 3). Most of the faults at trench 2 are sealed by unit C, D or E. Only fault 2, cuts unit D slightly, but clearly.



**Table 3.** Radiocarbon Dating Results<sup>a</sup>

Sample	Material	Unit/Trench	C13/C12 (0/00)	<sup>14</sup> C Age, years B.P.	Calibrated Age (2σ Interval)	<sup>13</sup> C/ <sup>12</sup> C, ‰
COLMENAR 1	silty layer	unit E, TR2	-21.0	2850 ± 70	1215–830 B.C.	-21
LORC 1–RC-1	silty layer	unit D, TR2	-22.6	3390 ± 40	1760–1600 B.C.	-22.6
LORC 2–RC-2	paleosoil	unit C (bottom), TR2	-21.9	15940 ± 50	17490–16670 B.C.	-21.9
LORC 3–RC-3	paleosoil	unit C (top), TR2	-22.0	3660 ± 30	2130–1945 B.C.	-22
TR4-RC2	shell	unit a, TR-4	-7.3	1350 ± 40	640–760 A.D.	-7.3
TR4-RC3	charcoal	unit a, in TR-4	-22.8	340 ± 40	1450–1650 A.D.	-22.8
TR4-RC8	silty layer	unit b, TR-4	-24.2	480 ± 40	1410–1460 A.D.	-24.2

<sup>a</sup>Sample TR4-RC3 was considered the best one for date units a and b at trench 4 given its charcoal nature.

[20] The yellowish red sediments of unit C differ from those of the rest of the stratigraphic units, which are gray in color. The only possible source for the red to yellow clays and silts of its matrix are the Neogene marls which crop out only in the hanging wall of the southeastern fault, downstream (inset map in Figure 4). The source area for the rest of the sediments at this site is the La Tercia range to the NW. Unit C is only located in the downthrown wall around Colmenar creek. Its location, reduced extension and low energy environment (fine-grained sediments) suggest that unit C results from the sudden damming of the southeastward drainage of Colmenar creek (or an earlier creek), possibly because of the uplift of the southeastern wall of the fault. Accordingly, the hills of the upthrown wall would therefore be the source of unit C (Figure 4).

[21] The internal deformation and tilting of units A to C and the abrupt sedimentary environmental change reflected by unit C were used as evidence of seismic events. There was evidence of at least two earthquakes, since the sedimentation of unit C. Earlier deformation can be observed but it could not be analyzed in terms of individual events.

#### 4.1.1. Event Z

[22] Assuming that unit C was deposited originally horizontal, its current NW dip suggests a tectonic tilting (observed at both trenches) caused by the reverse slip of the southeastern fault. This deformation occurred after the deposition of unit C but before the formation of unit E, which is not tilted. Independent evidence of a deformation event is provided by the ruptured bottom of unit D, which is affected by fault 2 (see magnification of trench 2). This event occurred after the deposition of unit D, which is deformed, and before the deposition of unit E, which seals the fault. Therefore, at least one event occurred between the deposition of unit C and E, i.e., between 1760 and 830 B.C. (Table 3). The seismic origin of this event is uncertain and should be corroborated by correlation with other events at different trenches.

#### 4.1.2. Event X

[23] This is evidenced by the nature of unit C, its southern origin, its local source, and its restriction to Colmenar creek, next to the fault. The relief produced by the reverse slip of the southern fault would have generated the damming of Colmenar creek and also the abrupt change in the source area. The stratigraphic lower limit of this unit is very sharp and suggests a sudden change in the environmental conditions. This event would have taken place just before the deposition of unit C (the change in sedimentary conditions is interpreted to be triggered by the movement of the fault and therefore little time is expected between the earthquake and the deposition of unit C) and long after the formation of

unit B (calcrete soil on top of alluvial fan A) which is the youngest deformed layer before unit C, i.e., between 35 ka and 16670 B.C. (but probably only a short time before 16670 B.C.).

## 4.2. Paleoseismic Studies at the El Saltador Site

[24] The slip of the fault across the El Saltador alluvial fan may also generate local damming. Trenches 3 and 4 (Figures 5 and 6) were dug across the smooth step generated by the fault at the El Saltador alluvial fan in an area where a small flat surface suggests the damming of a small gully (topographic map in Figure 6). See the topographical profile on the surface of the alluvial fan, across the fault, at the El Saltador site (profile P2 in Figure 3). Trench 3 was dug midway between the depocenter of the dammed area and its northeastern edge in order to avoid the possible erosion of the stream. Trench 4 was dug at the depocenter of the dammed area where, occasionally, previous damming events could have been recorded even if they had been of low intensity.

[25] Trench 3 (Figure 5) shows loose gravels interbedded with relict soil units (H, F and D), which form part of the El Saltador fan (Intermediate alluvial fan). Because of the direction of sediment transport from the La Tercia range toward the Guadalentín depression, the fan originally dipped slightly to the SE. This sedimentary dip (units I to C) is preserved in the northwestern half of the trench on both walls, but these units dip slightly to the NW, from meter 17 to 23, showing the bend of all these units. In the southeastern part of the trench, unit J, composed of moderately cemented gravels, dips to the northwest in an opposite direction to the fan slope. This unit shows an eroded and incompletely developed calcic soil on top. The uppermost part of the trench is filled with a fine-grained unit (B) northwest of the deformed area. This unit is located under the flat surface observed at the topographic level (meters 0 to 21). This trench reveals two deformation zones (correlatable between the two walls). The northern one (1 in Figure 5) consists of a set of reverse faults with centimetric offsets and angular folds. The axial planes of the angular folds and the reverse faults dip to the SE. This deformation affects only the lower sedimentary units of the trench (unit I). The southern deformation area (2 in Figure 5) consists of a gentle fold cut by a set of reverse faults, which are nearly vertical, but locally dipping SE, and show offsets in the order of few centimeters. These structures deform sedimentary units younger than those deformed in zone 1, and affect unit D. Between deformation zones 1 and 2 the layers dip to the NW. The interbedded soils are partly eroded by the overlying units. A number of unconformities

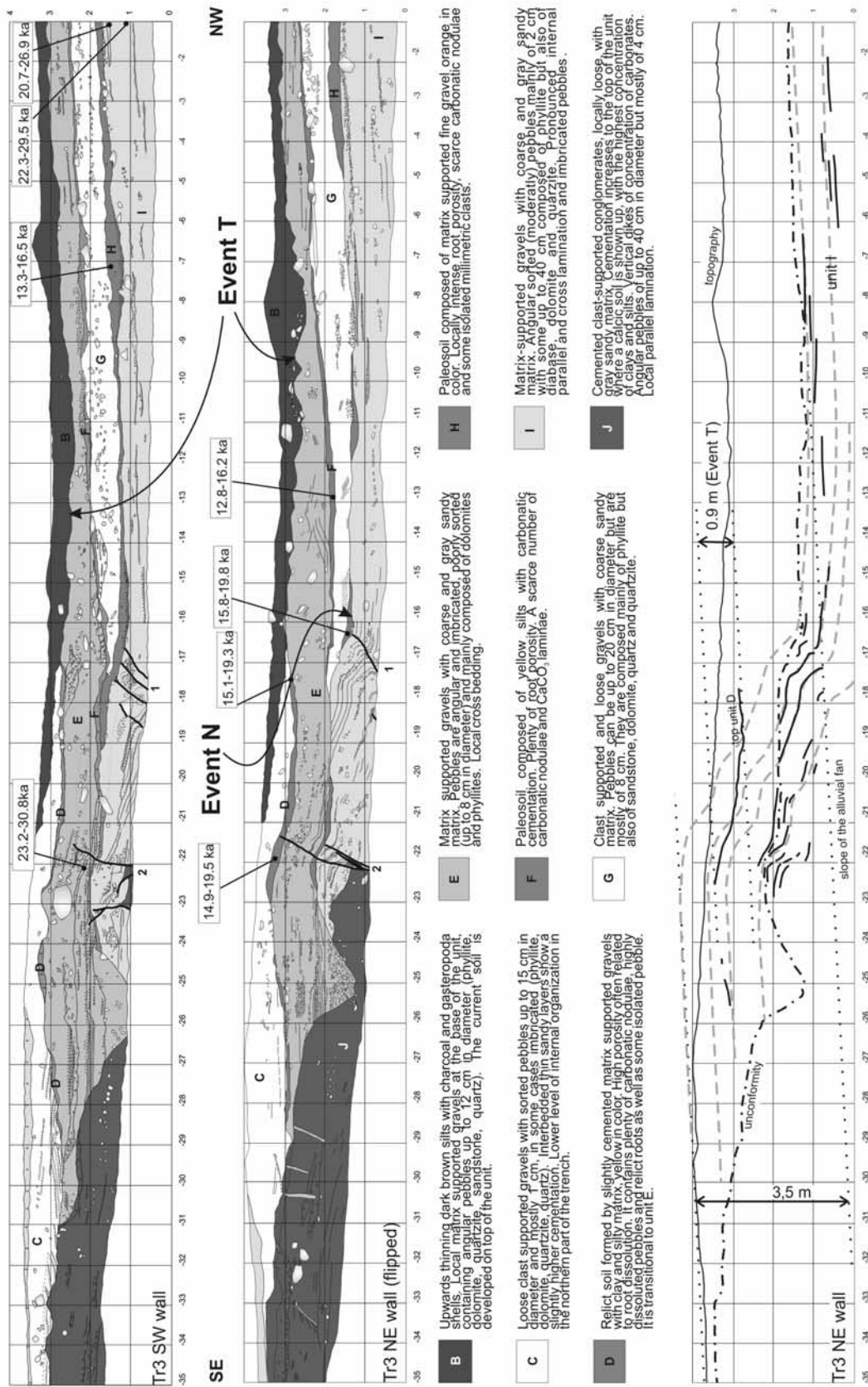


**Figure 5.** Geological cross section of the two walls of trench 3 (El Saltador site). See Figures 3 and 6 for location. Samples dated by thermoluminescence are labeled. Bottom log shows the vertical offset generated by events T and N estimated after restoring the eroded beds. Event T generated 0.9 m of vertical offset while event(s) N show 2.5 m of cumulative offset (3.5 m minus the 0.9 m of event T).

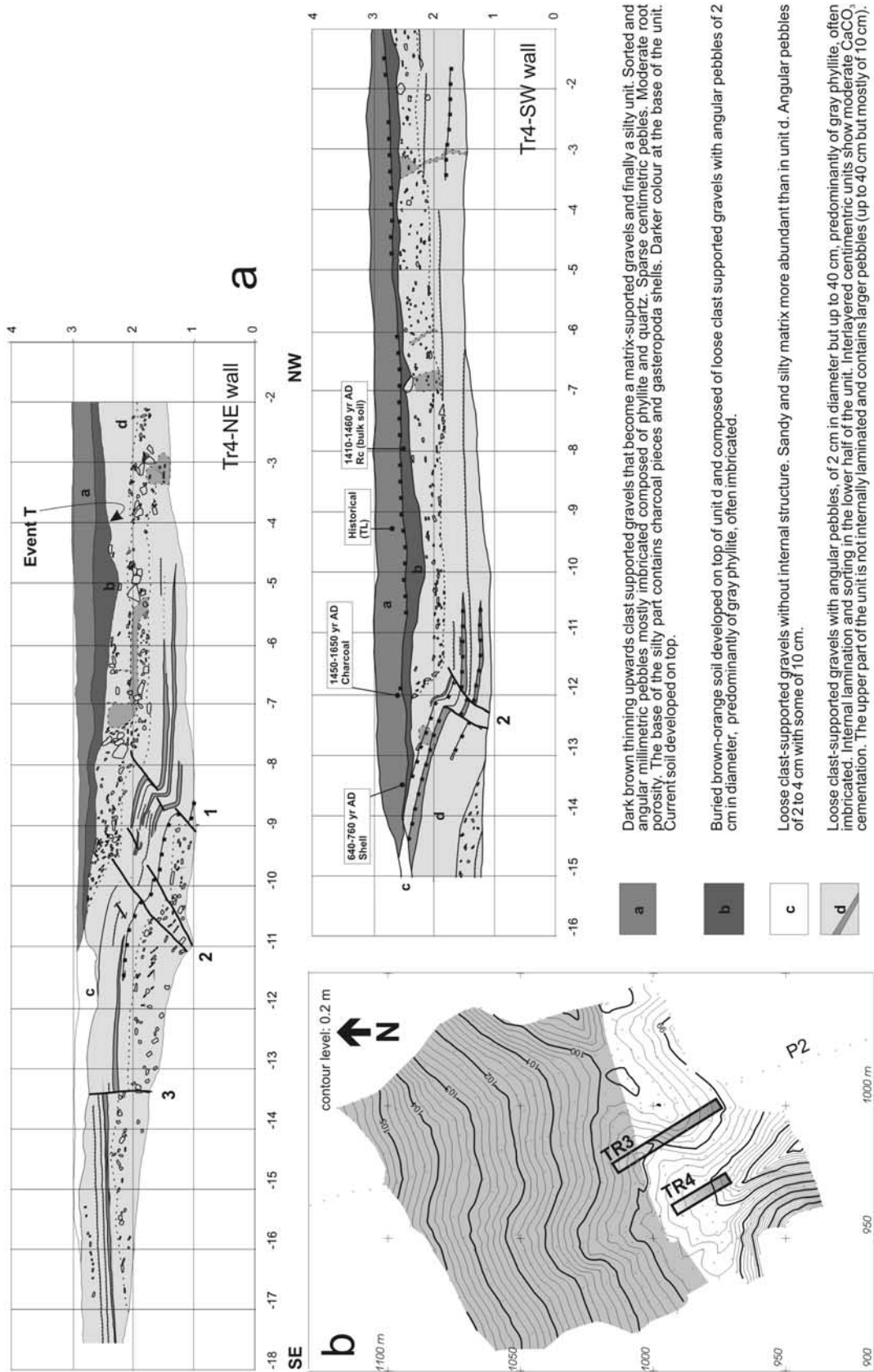


**Figure 6.** (a) Geological cross sections of trench 4 (El Saltador site). Samples labeled were dated by radiocarbon except for that labeled with (TL) for which the thermoluminescence pretreatment suggested a historical age. See Figure 3 for location. (b) Microtopographic map of the El Saltador site with location of the trenches 3 and 4. Note the flat surface on foot of the fault scarp and in coincidence with the small stream. It corresponds to the area where unit B was deposited.

occur at the bottom of most of the units (bottoms of units G, E, C, and B). These units lie on truncated beds over the deformed zones, whereas away from these zones they are parallel to the underlying beds.

[26] Trench 4 (Figure 6) shows two main units: the alluvial fan sediments (d), and the fine-grained sediments (a, b, and c), which are on top. Units a and b can be distinguished because of their differences in color and gravel content, which can be attributed to small changes in the flow energy. The trench shows three areas of deformation: Zone 1 consists of a decimeter size folding with a kink-band pattern with local dislocations along the fault planes that produce vertical offsets of the layers. These structures affect unit d but do not involve units c, b, and a. Zone 2 has characteristics similar to those of zone 1. Zone 3, the southernmost deformation feature in this trench, is a vertical fault with a clear offset and does not show folding. Between the deformation zones, the bedding dips to the NW and to the southeast of zone 3 the layers recover their original SE dip of the fan. Units c, b, and a unconformably overlie unit d, cutting several of its beds, in the deformation zones whereas at some distance they become parallel to d, indicating the tectonic origin of the unconformity.

[27] At least two deformation events can be identified at this site according to the following evidence: (1) abrupt change in the type of deposition (from gravels to clays) attributed to the damming of the drainage by the fault movement and deposition of these fine sediments in coincidence with the newly formed scarp, and (2) unconformity located over deformed zones (faults and folds) separating groups of sedimentary units which are equally deformed.

#### 4.2.1. Event T

[28] Units B (trench 3) and b (trench 4) are correlatable and represent the sedimentary record of a possible damming episode of the southward drainage of the gully. The B, b unit is located under the flat surface of the area adjacent to the fault. It is clearly linked to the deformed zone as revealed by the trench logs: its depositional limit to the south is located over the youngest deformation structure at trench 3 (fault zone 2) and at trench 4 (deformed zones 2 and 3). Its sharp lower limit also suggests an abrupt change in the sedimentary conditions that are attributed to a sudden uplift of the southeastern block of the fault, i.e., an earthquake. Bending of units E, D, and C at trench 3 over fault zone 2 also account for this event. Absolute dating of the bottom of unit a at trench 4 (results obtained from charcoal were preferred rather than from soil or shell, see Table 3) and of unit D at trench 3 bracket the age of this earthquake between 16.2 ka and 1650 A.D. (Figure 7). Although the bracket is very wide, the best estimate is very close to the youngest age given that the damming was an immediate consequence of the earthquake. Accordingly, the possibility of the historical occurrence of event T was taken into account.

#### 4.2.2. Event N

[29] The bottom of unit H at trench 3 covers: (1) fault zone 1, (2) part of the deformation at fault zone 2, and (3) the truncated internal laminations of unit I. Therefore event horizon N is possibly located at the bottom of unit H. Absolute dating of units H and I indicate a time bracket for this event between 26.9 and 15.8 ka.

[30] The vertical offset of unit D (affected only by event T) is 0.9 m (Figure 5). The minimum vertical offset observed in

the layering within unit I (affected by events T and N) after restoring the erosion is 3.5 m. Subtracting the offset attributed to event T from this value, the amount of vertical offset of event N results in 2.5 m and it is much larger than that observed for event T (0.9 m). This suggests that N could be a multiple event (at least three if the 0.9 m slip per event is accepted). After restoring the deformation produced by event T, unit H still shows a nonplanar shape in fault zone 2 (southern wall of trench 3) and in fault zone 1 (trench 3). This suggests that this soil (H) was developed over a partly eroded old fault scarp. The small paleohill was buried by onlapping of younger units G, E and C, which were probably episodic and separated in time as evidenced by the soils developed on top of them (units F and D).

### 4.3. Correlation of the Events and Paleoseismic Parameters of the Lorca-Totana Segment

[31] This paleoseismic study provides evidence of two possible past earthquakes at each site. The events were defined on the basis of the following evidence: (1) sudden change in sedimentation conditions (from alluvial to stream damming environments) associated with deformed sediments (event T, El Salvador), (2) unconformities separating layers with different degrees of deformation (event N, El Salvador), (3) tilting of a layer interpreted to be formed horizontally (event Z, Colmenar), and (4) sedimentary unit (unit C at the Colmenar site) deposited only next to the fault and showing evidence of sudden shift of the source area, from the La Tercia range (general source area for the zone) to the relief generated by the movement of the fault downstream (event X, Colmenar).

[32] Figure 7 shows the time bracket for each of these events. Bearing in mind that only a minimum number of the real large events are recorded, the correlation between events detected at the two sites is not obvious. However, the correlation between events T and Z is possible because the time bracket for event Z is included in the time bracket for event T. A number of possibilities can be considered: (1) events T and Z correlate and therefore event T is not historical (the oldest registered historical earthquake in the area occurred in 1579 I = VII with the epicenter in Lorca, whereas the youngest limit for event Z is 830 B.C.), (2) events T and Z correspond to two different events (rupture of T did not affect the Colmenar site and rupture of Z did not affect the El Salvador site), and (3) there are two events recorded at each site but they cannot be separated. A large earthquake at Colmenar would possibly rupture at El Salvador, and vice versa, because both sites belong to the same segment of the Alhama de Murcia fault; therefore, option 2 is improbable. Bearing in mind that event T is likely to have occurred shortly before the deposition of unit B (silts are the result of damming), the correlation between this and event Z (option 1) is difficult. However, it is unlikely that the historical 1579 A.D. event in Lorca was event T given its low intensity values. Conversely, we prefer option 3 because only some earthquakes could be geologically recorded.

[33] The best estimate for event X also corresponds to the youngest part of its time bracket (see section 4.1). Therefore event X could constitute one of the events composing multievent N.

[34] In conclusion, events T-Z could correspond to two events and occurred between 1650 A.D. and 1760 B.C. (best

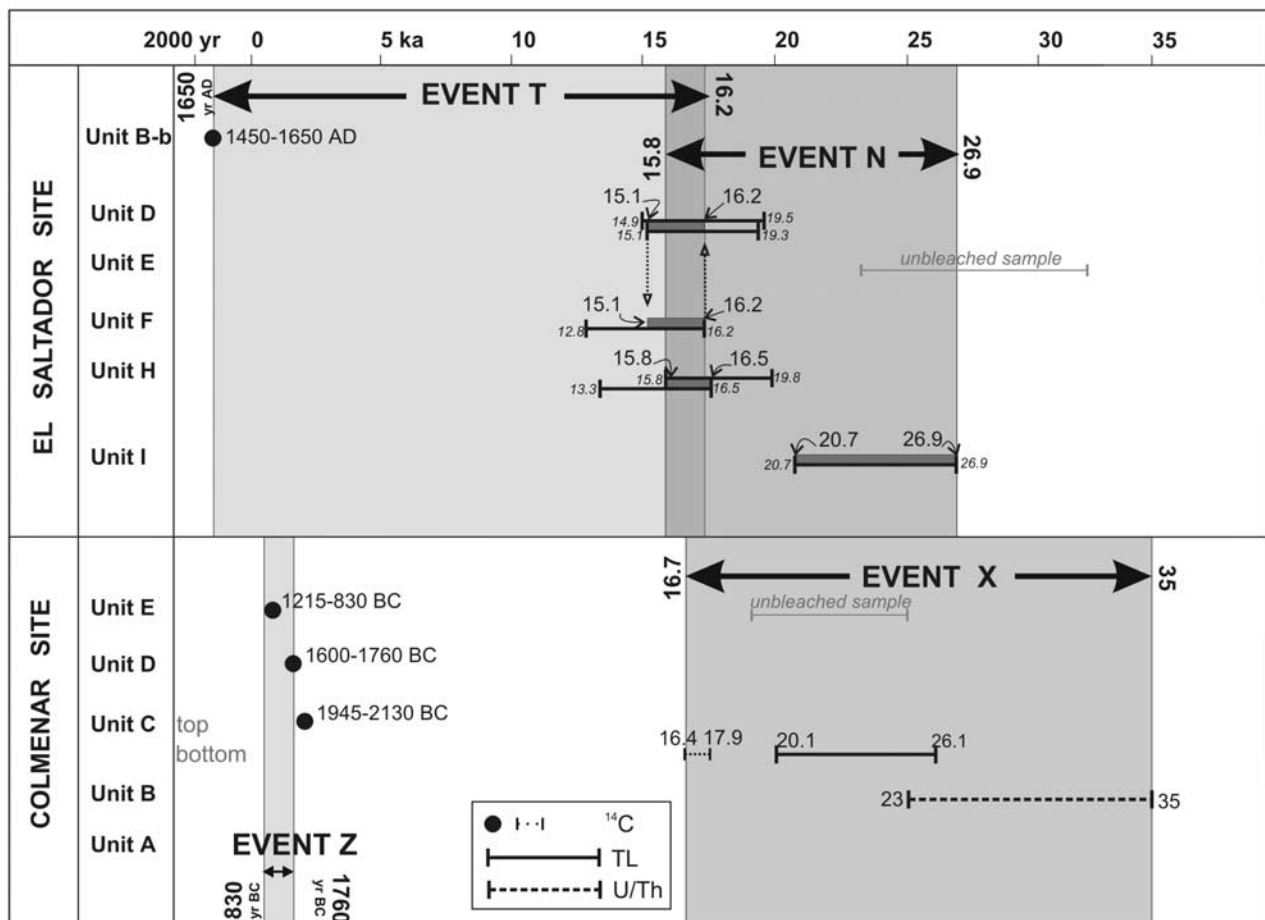


**Figure 7.** Dating results obtained for each of the units sampled (values in small italic letters). Best estimate for each unit is indicated by a dark gray strip with ages in large black labels. Complete time bracket for the earthquakes detected at each site is provided. Samples labeled in light gray are not considered in the discussion because of their inconsistent results (not geologically consistent, such as lower layers being younger than upper). At the El Saltador site, the oldest possible age of unit D cannot be older than the oldest age of the underlying unit F. Therefore the same age was attributed to the lower limit of unit D and to unit F, although samples dated in unit D provide older ages. The same stratigraphic reasoning was used to constrain the age of the top of unit F with the result that the age bracket for both units (D and F) coincides.

estimate for the occurrence of event T is little time before 1650 A.D. and of event Z between 830 and 1760 B.C.) and event N-X around 16.7 ka. Therefore the average maximum time period between events T, Z and N-X is  $\sim 14$  kyr if three events are considered and the elapsed time since the last event is very small by comparison. Note that the recurrence period is not regular when taking into account three events: the time between the two last events is shorter (2000) than between the penultimate and the old event suggesting clustering.

[35] Events T and Z could correspond to a sudden event (i.e., earthquake), given (1) the fine-grained nature of the sediments of units B/b-a (trench 3/trench 4) and C (trenches 1 and 2) related to a damming process triggered by the fault dislocation, (2) the sharp bottom contact of these units over the coarse deposits of the fans, and (3) the change of the source area (unit C at trenches 1 and 2). There is no direct evidence for a seismic nature of event N-X. However, historical data suggest a seismogenic behavior of

the Alhama de Murcia fault and we interpret this event as seismic although creep cannot be excluded.

[36] The vertical component of the slip rate was calculated by using the available ages of the alluvial fan layers and the vertical offsets which were obtained from two sources: (1) the vertical slip per event measured at the trenches and (2) the microtopographic profiles performed along the alluvial fans of known age. Only trench 3 provided data on the vertical coseismic offset, which is 0.9 m for event(s) T (Z) (0.45 m if two events are considered) and 2.5 m for events N (Figure 5). Therefore the cumulative vertical offset at this site is 3.5 m, during, at least, the last  $23.8 \pm 3.1$  kyr (age of top of unit I at trench 3, just below the unconformity, see Table 4), which results in a vertical slip rate of 0.12–0.16 mm/yr. The slip rate, however, is much lower for the last  $17.2 \pm 2.3$  kyr (age of unit D at trench 3, below silty sediments of unit B): 0.04–0.06 mm/yr.

[37] The surface of the El Saltador alluvial fan is offset 2 m (profile P2 in Figure 3) and the available age of the

**Table 4.** Thermoluminescence and U/Th Dating Results

Sample	Thermoluminescence	
	Unit/Trench	TL Age, ka
TRM47	unit C/Tr2	23.1 ± 3.0
TRM27	unit D/Tr3	17.2 ± 2.1
TRM43	unit D/Tr3	17.2 ± 2.3
TRM45	unit E/Tr3	27.0 ± 3.8
TRM49	unit E/Tr2	22.2 ± 3.2
TRM41	unit F/Tr3	14.5 ± 1.7
TRM24	unit H/Tr3	14.9 ± 1.6
TRM54	unit H/Tr3	17.8 ± 2.0
TRM21	unit I/Tr3	23.8 ± 3.1
TRM56	unit I/Tr3	25.4 ± 3.1

<sup>234</sup> U/ <sup>238</sup> U	<sup>231</sup> Th/ <sup>234</sup> U	Number of Points for Isochron	R <sup>2</sup>	U/Th Age, years
1.6968	0.2388	4	0.93	29064 (+6517–6195)

uppermost layer of the fan is  $17.2 \pm 2.3$  ka (oldest estimated age of layer D in TR3, see Figure 7), which indicates a 0.10–0.13 mm/yr maximum vertical slip rate (possible inherited fault scarp could produce overestimation of this value). In the Colmenar fan 8 m of vertical offset were measured by combining the topographic profile (profile P1 in Figure 3) and the location of the top of the alluvial fan observed at trench 1. U/Th dating of the calcete soil on top of this fan provided an age of  $29 \pm 6$  ka for the soil (Table 4). This implies a maximum vertical slip rate of 0.35 mm/yr. Bearing in mind the time needed to develop such a laminated calcic soil (the age of the sediment is older than that of the soil), these slip rate values should be regarded as an overestimation. The obtained vertical slip rate values (0.10–0.35 mm/yr) correspond to the last 30 kyr of the history of the fault. This is very similar to that obtained since the Tortonian (6–11 Myr) estimated in neotectonic studies by *Martínez-Díaz and Hernández Enrile* [1996], which ranges between 0.14 and 0.27 mm/yr. The slip rate obtained for the most recent period, however, suggests a decrease in the slip rate (0.04–0.06 mm/yr).

[38] The strike slip component of the fault can reach values higher than those of the vertical slip owing to the

slickensides observed at the trenches (pitch from  $32^\circ$  to  $60^\circ$ ). Considering a pitch of  $32^\circ$  (to obtain the highest possible rates), the net slip rate varies between 0.07 and 0.66 mm/yr and the strike slip rate between 0.06 and 0.53 mm/yr (Table 5). Note, again, that the upper values are probably overestimated since they were obtained from the age of the soil developed on top of the offset surface.

[39] The length of the analyzed southern fault is at least 10 km (shorter than the complete Lorca-Totana segment in which it is included). The thickness of the seismogenic layer in this part of the Iberian Peninsula is considered to be 12–15 km according to the depth of the seismicity [*Martínez-Díaz, 1998*]. Following *Wells and Coppersmith* [1994], the rupture of a 150 km<sup>2</sup> area can generate an earthquake of  $M_w$   $6.1 \pm 0.01$  ( $M_w$   $6.3 \pm 0.1$  if the whole 16 km long segment is considered). The magnitude can also be estimated from the coseismic offset. The 0.9 m of vertical offset correspond to 1–1.7 m of net slip ( $32^\circ$ – $60^\circ$  pitch) and this to  $M_w$  6.7–7.0 ( $\pm 0.04$  and  $\pm 0.1$ , respectively). However, if two events T and Z are considered, the equivalent  $M_w$  is 6.6–6.7 ( $\pm 0.1$  and  $\pm 0.04$ ). The higher values obtained from the coseismic offset (even when two events are considered) suggest the possibility of past seismic rupture across segment boundaries. Therefore, although the data are still weak on this point, the complete rupture of the fault producing a single earthquake cannot be ruled out.

## 5. Seismotectonic Implications

[40] Comparison of the slip absorbed by the known seismogenic faults located on the boundary between African and Iberian plates with the convergence slip rates raises a number of questions concerning the seismotectonics of this region. A transect is considered parallel to the convergence vector whose azimuth varies between  $N125^\circ$  and  $E160^\circ$  depending on the different approaches [*Argus et al., 1989; DeMets et al., 1990, 1994; McClusky et al., 2003; Galindo-Zaldívar et al., 1993; Kiratzi and Papazachos, 1995*]. The 4.5–5.6 mm/yr convergence rates estimated by plate motion models [*Dewey et al., 1989; Argus et al., 1989; DeMets et al., 1990, 1994*] resembles the values obtained by

**Table 5.** Vertical Offset and Age of the Alluvial Fans at Different Sites Along the Alhama de Murcia Fault<sup>a</sup>

	Vertical Offset, m	Age, ka	Vertical Slip Rate, mm/yr	Net Slip Rate, mm/yr	Strike-Slip Rate, mm/yr	Shortening Along N160° Transect, mm/yr
Trench 3 ( $17.2 \pm 2.3$ ka)	0.90	$17.2 \pm 2.3$	0.04–0.06	0.07–0.11	0.06–0.09	0.05–0.08
Trench 3 ( $23.8 \pm 3.1$ ka)	3.5	$23.8 \pm 3.1$	0.12–0.16	0.23–0.3	0.18–0.24	0.16–0.22
El Saltador fan	<2 <sup>b</sup>	$17.2 \pm 2.3$	0.10–0.13	0.19–0.24	0.15–0.20	0.14–0.18
Colmenar fan	8.0	< $29 \pm 6$ <sup>c</sup>	<0.23–0.35	<0.43–0.66	<0.35–0.53	<0.31–0.48
				Slip Rate Along a N160° Transect, mm/yr	Total Shortening, %	
Total Africa-Iberia shortening rate				4.5–5.5		
Estimated shortening rate at the Iberian margin (along faults)				0.15–1.4		2–31
Estimated shortening rate at the African margin (along faults)				1–2.3		18–51
Total shortening rate along seismogenic faults				1.15–3.7		21–82

<sup>a</sup>Vertical, net, and strike-slip rates are obtained from these by considering a vertical fault and a pitch of  $32^\circ$  (measured pitch ranges between  $32^\circ$  and  $60^\circ$ ;  $32^\circ$  was selected here to obtain the maximum possible rates). The age labeled for the Colmenar fan (lowest value of the range  $29 \pm 6$  ka) is a minimum because it was obtained from the dating of the calcic soil on top of this surface. Shortening absorbed by the Alhama de Murcia fault ( $N050^\circ E$ ) is measured along a  $160^\circ$  shortening direction (see text for further discussion). Shortening values are shown for each plate margin (African values by *Morel and Meghraoui* [1996]) as annual slip rate and as percentage of the plate motion values [*Argus et al., 1989*].

<sup>b</sup>May be overestimated.

<sup>c</sup>Possibly underestimate.

GPS measuring although these are slower: 4.5 mm/yr [McClousky *et al.*, 2003]. The seismic moment tensor summation also indicates a 4.5 mm/yr of coseismic crustal shortening rate along this transect [Kiritzi and Papazachos, 1995] although this value is probably overestimated by the amount of seismic moment provided by the recent El Asnam earthquake in Algeria (1980).

[41] Few known seismogenic faults are cut by the NNW-SSE transect, which includes the Lorca-Totana segment. These are, from north to south, in the Iberian plate the Crevillente, the Alhama de Murcia and the Carrascoy-Palomares fault systems [Sanz de Galdeano, 1990; Buforn *et al.*, 1995] and in the African plate, the prolongation to the east of the Yussuf fault [Alvarez-Marrón, 1999], the Oued Allalah thrust with a Quaternary vertical slip rate of 0.5 mm/yr [Aoudia and Meghraoui, 1995] and the Oued Fodda Fault that generated the El Asnam earthquake [Philip and Meghraoui, 1983; Mauffret *et al.*, 1987; Swan, 1988; Mauffret *et al.*, 1992; Meghraoui and Doumaz, 1996; Morel and Meghraoui, 1996]. Some other faults with Quaternary activity have been described in the Alboran sea (i.e., the Alboran ridge, and the Yussuf fault). These are not considered here since their seismogenic behavior is poorly constrained [Woodside and Maldonado, 1992; Watts *et al.*, 1993; Comas *et al.*, 1999] and they are mostly located to the west of the chosen transect.

[42] The geomorphological expression of the Alhama de Murcia fault is comparable to that of the Carrascoy-Palomares fault and is slightly more marked than that of the Crevillente fault. Therefore their slip rates could also be comparable. The Alhama de Murcia fault has a 0.05–0.48 mm/yr shortening rate along a N160E transect parallel to the direction plate convergence (Table 5). Assuming a similar value for all these faults in the Iberian plate, a 2–31% of the total shortening between both plates is absorbed by this Iberian sector. A higher value (0.4–0.6 mm/yr) has been attributed to the El Asnam fault [Morel and Meghraoui, 1996] and to the Rif and Tell geological domains (1–2.3 mm/yr), where several northeast-southwest trending folds such as the Oued Allalah thrust show a morphological expression similar to that of the El Asnam [Morel and Meghraoui, 1996]. In line with this assumption the Tell and the Iberian known faults would absorb only the 21–82% of the total shortening between the two plates (Table 5). Note that the 82% is an overestimation since it was obtained from the Colmenar slip rate.

[43] A number of factors could account for the unexplained shortening: (1) The Alhama de Murcia fault could be one of the slowest faults in the Iberian sector with the result that the other slip rates have been underestimated when extrapolating the results of this fault to them. (2) Other seismogenic faults could occur offshore. (3) Some long active faults could behave aseismically. (4) Other large seismogenic faults could occur onshore. (5) The large number of small faults, which characterize the diffuse boundary and which do not produce large earthquakes, could absorb a significant part of the shortening. (6) The current convergence rate could not be representative of the mean shortening rate of the last 30 kyr. (7) The convergence rates are overestimated.

[44] We rule out the first two factors for the following reasons: i) The morphological expression of the Alhama de Murcia fault is one of the best preserved in the eastern

Betics. Consequently, it is unlikely that its slip rate is one of the lowest of the active faults in this area. ii) The epicenter distribution suggests that most of the deformation is absorbed onshore (although this possibility can not completely be rejected according to the  $M_w$  6.8 May 21 2003 Algerian earthquake whose epicenter was located several km offshore).

[45] The remaining factors are more likely to account for the discrepancy in different degrees. Other seismogenic faults could exist onshore since a compilation of the neotectonic structures in areas of slow moving faults could overlook those faults which have not yet been released by an earthquake. Widespread faults could absorb deformation without generating evident geomorphological features, and could therefore be scarcely detectable. As suggested at trench 3, clustering of the seismic events or changes in the slip rate should also be born in mind. Finally, although the seismic moment summation and the plate convergence seems coherent, aseismic faulting cannot be rejected given the possible overestimation of the seismic moment summation generated by the El Asnam earthquake.

## 6. Conclusions

[46] The Lorca-Totana segment of the Alhama de Murcia fault is seismogenic and has generated a minimum of two, and very probably three, large earthquakes in the last 27 kyr, the last one (event T) being very recent (shortly before 1650 A.D.), which is probably not the 1579 Lorca earthquake (MSKI = VII) given the low intensity of the latter. The previous event (Z) occurred between 830 and 2130 B.C., and the oldest (possibly a multiple event, N-X) took place shortly before 16.7 ka. The average recurrence period is of 14 kyr (with evidence for clustering: the time between the last two earthquakes would be of 2 kyr) and the elapsed time is short in comparison. The maximum magnitude of this fault varies from  $M_w$  6.1 to 7.0 depending on whether the rupture area or the slip per event is used to estimate it and also depending on whether the events T and Z are regarded as two different earthquakes. Accordingly, the complete rupture of the Alhama de Murcia fault across the defined segments cannot be ruled out. The fault shows an oblique left lateral/reverse slip. The vertical slip rate is 0.04–0.35 mm/yr, and the estimated strike and net slip rates are 0.06–0.53 mm/yr and 0.07–0.66 mm/yr, respectively.

[47] The amount of convergence absorbed by the seismogenic faults across the Iberian margin ranges probably between 0.15 to 1.4 mm/yr, which is 2–31% of the total shortening between Africa and Iberia estimated from plate motion models and seismic moment additions. This amount, together with that estimated for the African plate, is only 21–82% of the total shortening. A number of factors could account for this discrepancy: (1) hidden seismogenic faults in the emerged areas were not taken into account, (2) absence of correlation between current and late Pleistocene slip rates, (3) extensive small faults that are undetected and that absorb a significant amount of the deformation, (4) aseismic faulting, and (5) overestimation of the convergence rates.

[48] **Acknowledgments.** The authors wish to thank J. Hernández-Enrile, sadly deceased during the development of this work, for his personality, friendship, and expertise. This study was sponsored by the FAUST project (ENV4-CT97-0528), SAFE project (EVG1-CT-2000-23),

and project B97-053 (CICYT). We are indebted to Mabel Gómez, Raquel Amores, Angel Martínez, Juan Arregui, Héctor Perea, and Juanmi Insua for their invaluable help in field work and discussions. Thanks are also due to Victoria Tejón for permission to trench on their properties. Thermoluminescence studies were carried out by N. Debenham (Quaternary TL Surveys), uranium series by R. Julià (Institut Jaume Almera, CSIC, Barcelona) and Radiocarbon dating by Beta analytics Inc. We are also grateful to H. Lyon-Caen, M. Sebrier and to an anonymous reviewer for their comments and suggestions.

## References

- Alfaro, P., J. Galindo-Zaldívar, A. Jabaloy, A. C. López-Garrido, and C. Sanz de Galdeano (2001), Evidence for the activity and paleoseismicity of the Padul fault (Betic Cordillera, southern Spain), *Acta Geol. Hispanica*, *36*, 283–295.
- Alvarez-Marrón, J. (1999), Pliocene to Holocene structure of the eastern Alboran Sea (Western Mediterranean), *Proc. Ocean Drill. Program Sci. Results*, *161*, 345–355.
- Amores, R., J. L. Hernández-Enrile, and J. J. Martínez-Díaz (2002), Estudio gravimétrico previo aplicado a la identificación de fallas ocultas como fuentes sismogénicas en la depresión del Guadalentín (Región de Murcia), *Geogaceta*, *32*, 307–310.
- Argus, D. F., R. G. Gordon, C. DeMets, and S. Stein (1989), Closure of the Africa-Eurasia-North American plate motion circuit and tectonics of the Gloria Fault, *J. Geophys. Res.*, *94*, 5585–5602.
- Armijo, R. (1977), La zone de failles Lorca-Totana (Cordillères Bétiques, Espagne). Étude tectonique et néotectonique, thèse 3ème cycle, Univ. Paris VII, Paris.
- Aoudia, A., and M. Meghraoui (1995), Seismotectonics in the Tellian Atlas of Algeria: The Cavaignac (Abou El Hassan) earthquake of 25 August 1922, *Tectonophysics*, *248*, 263–276.
- Baena, J., L. M. Barranco, C. Zazo, J. L. Goy, P. G. Silva, L. Somoza, T. Bardaji, A. Estévez, C. Sanz de Galdeano, and T. Rodríguez (1993), Mapa neotectónico sismo-tectónico y de actividad de fallas de la Región de Murcia, Cons. de Cultura y Educ., Comun. Auton. de la Reg. de Murcia, Madrid.
- Bousquet, J. C. (1979), Quaternary strike-slip faults in southeastern Spain, *Tectonophysics*, *52*, 277–286.
- Bousquet, J. C., and C. Montenat (1974), Presence de décrochements Nord Est - Sud Ouest plio-quaternaires dans les Cordillères bétiques orientales (Espagne): Extension et signification générale, *C. R. Acad. Sci.*, *278*, 2617–2620.
- Bousquet, J. C., C. Montenat, and H. Philip (1978), La evolución tectónica reciente de las Cordilleras Béticas orientales, in *Reunión Geodinámica de la Cordillera Bética y Mar de Alborán*, 1976, pp. 59–78, Secret. de Publ., Univ. de Granada, Granada, Spain.
- Bufo, E., A. Udías, and R. Madariaga (1991), Intermediate and deep earthquake in Spain, *Pure Appl. Geophys.*, *136*, 375–393.
- Bufo, E., C. Sanz de Galdeano, and A. Udías (1995), Seismotectonics of the Ibero-Maghrebian region, *Tectonophysics*, *248*, 247–261.
- Comas, M. C., J. P. Platt, J. J. Soto, and A. B. Watts (1999), The origin and tectonic history of the Alboran Basin: Insights from leg 161 results, *Proc. Ocean Drilling Program Sci. Results*, *161*, 555–580.
- Crone, A. J., M. N. Machette, and J. R. Bowman (1997), Episodic nature of earthquake activity in stable continental regions revealed by paleoseismicity studies of Australian and North American Quaternary faults, *Aust. J. Earth Sci.*, *44*, 203–214.
- Cung, W., and H. Kanamori (1976), Source process and tectonic implications of the Spanish deep-focus earthquake of 29 March 1954, *Phys. Earth Planet. Inter.*, *13*, 85–96.
- D'Addezio, G., F. R. Cinti, and D. Pantosti (1995), A large unknown historical earthquake in the Abruzzi region (central Italy): Combination of geological and historical data, *Ann. Geofis.*, *38*, 491–501.
- DeMets, C., R. G. Gordon, D. F. Argus, and S. Stein (1990), Current plate motions, *Geophys. J. Int.*, *101*, 425–478.
- DeMets, C., R. G. Gordon, D. F. Argus, and S. Stein (1994), Effect of recent revisions to the geomagnetic reversal time scale on estimate of current plate motions, *Geophys. Res. Lett.*, *21*, 2191–2194.
- Dewey, J. F., M. L. Helman, E. Turco, D. H. W. Hutton, and S. D. Knot (1989), Kinematics of the western Mediterranean, in *Alpine Tectonics*, edited by M. P. Coward, D. Dietrich, and R. G. Park, *Geol. Soc. Spec. Publ.*, *45*, 265–283.
- Doblas, M., and R. Oyarzun (1989), Neogene extensional collapse in the western Mediterranean (Betic-Rif Alpine orogenic belt): Implications for the genesis of the Gibraltar arc and magmatic activity, *Geology*, *17*, 430–433.
- Galindo-Zaldívar, J., F. González-Lodeiro, and A. Jabaloy (1993), Stress and paleostress in the Betic-Rif cordilleras (Miocene to the present), *Tectonophysics*, *227*, 105–126.
- Gauyau, F., R. Bayer, J. C. Bousquet, J. C. Lachaud, A. Lesquer, and C. Montenat (1977), Le prolongement de l'accident d'Alhama de Murcia entre Murcia et Alicante (Espagne méridionale). Résultats d'une étude géophysique, *Bull. Soc. Géol. Fr., Sér. 7*, *19*, 623–629.
- Grimson, N., and W. Cheng (1986), The Azores-Gibraltar plate boundary: Focal mechanisms, depths of earthquakes and their tectonic implications, *J. Geophys. Res.*, *91*, 2029–2047.
- Instituto Geográfico Nacional (IGN) (2001), Catálogo Sísmico Nacional hasta el 2001, Madrid.
- Kiratzi, A., and C. B. Papazachos (1995), Active crustal deformation from the Azores triple junction to the Middle East, *Tectonophysics*, *243*, 1–24.
- Lonegan, L., and N. White (1997), Origin of the Betic-Rif mountain belt, *Tectonics*, *16*, 504–522.
- López, C., A. Estévez, J. A. Pina, and C. Sanz de Galdeano (1987), Alineaciones sismotectónicas en el sudeste de España. Ensayo de delimitación de fuentes sísmicas, *Mediterranea, Ser. Geol.*, *6*, 5–38.
- López, C., C. Sanz de Galdeano, J. Delgado, and M. A. Peinado (1995), The b parameter in the Betic Cordillera, Rif and nearby sectors. Relations with the tectonics of the region, *Tectonophysics*, *248*, 277–292.
- López Marinas, J. M. (1977a), Historical earthquakes in Almería, internal report, Hidroeléctrica Española, Madrid, Spain.
- López Marinas, J. M. (1977b), Historical earthquakes in Murcia, internal report, Hidroeléctrica Española, Madrid, Spain.
- López Marinas, J. M. (1978), Terremotos históricos acaecidos en las provincias de Murcia y Alicante, *Cimbra, Rev. Ing. Tec. Obras Publ.*, *155*, 4–16.
- Martínez-Díaz, J. J. (1998), Neotectónica y tectónica activa del sector centro-occidental de la región de Murcia y sur de Almería (Cordillera Bética, España), tesis de doctorado, Univ. Complutense, Madrid.
- Martínez-Díaz, J. J. (2002), Stress field variation related to fault interaction in a reverse oblique-slip fault: The Alhama de Murcia fault, Betic Cordillera, Spain, *Tectonophysics*, *356*, 291–305.
- Martínez-Díaz, J. J., and J. L. Hernández-Enrile (1992a), Fracturación y control tectosedimentario neógeno en el borde Sureste de la cuenca de Lorca, *Bol. Geol. Minero*, *103*, 971–983.
- Martínez-Díaz, J. J., and J. L. Hernández-Enrile (1992b), Tectónica reciente y rasgos sismotectónicos en el sector Lorca-Totana de la falla de Alhama de Murcia, *Estad. Geol.*, *48*, 153–162.
- Martínez-Díaz, J. J., and J. L. Hernández-Enrile (1996), Origen y evolución neotectónica de la Sierra de La Tercia. Contribución a la segmentación tectónica de la falla de Alhama de Murcia, paper presented at VI Congreso Nacional y Conferencia Internacional de Geología Ambiental y Ordenación del Territorio, Univ. de Granada, Granada, Spain.
- Martínez-Díaz, J. J., and J. L. Hernández-Enrile (1999), Segmentación tectónica de la falla de Alhama de Murcia y actividad paleosísmica asociada. Contribución a la determinación de la peligrosidad sísmica en la región de Murcia, in *1er. Congreso Nacional de Ingeniería Sísmica. Memorias*, vol. Ia, pp. 75–87, Assoc. Española de Ing. Sísmica, Murcia, Spain.
- Martínez-Díaz, J. J., E. Masana, J. L. Hernández-Enrile, and P. Santanach (2001), Evidence for coseismic events of recurrent prehistoric deformation along the Alhama de Murcia fault, southeastern Spain, *Acta Geol. Hispanica*, *36*, 315–327.
- Martínez-Guevara, J. B. (1984), Temblores de tierra del núcleo sísmico de Lorca-Totana (Murcia): Estudio de sismicidad histórica, internal report, Inst. Geogr. Nac., Madrid.
- Martínez Solares, J. M., and J. Mezcuca (2002), Catálogo sísmico de la Península Ibérica (880 a.c.–1900), *Monografía 18*, 253 p., Inst. Geogr. Nac., Madrid.
- Masana, E. (1996), Evidence for past earthquakes in an area of low historical seismicity: The Catalan coastal ranges, NE Spain, *Ann. Geofis.*, *39*, 689–704.
- Masana, E., J. A. Villamarín, and P. Santanach (2001), Paleoseismic results from multiple trenching analysis along a silent fault: The El Camp fault (Tarragona, northeastern Iberian Peninsula), *Acta Geol. Hispanica*, *36*, 329–354.
- Mauffret, A., M. El-Robrini, and M. Gennesseaux (1987), Indice de la compression récente en mer Méditerranée: Un bassin losangique sur la marge nor-algérienne, *Bull. Soc. Géol. Fr.*, *8*, 1195–1206.
- Mauffret, A., A. Maldonado, and A. C. Campillo (1992), Tectonic framework of the eastern Alboran and western Algerian Basins, western Mediterranean, *Geo Mar. Lett.*, *12*, 104–110.
- McClusky, S. R., R. Reilinger, S. Mahmoud, D. Ben Sari, and A. Tealeb (2003), GPS constraints on Africa (Nubia) and Arabia plate motions, *Geophys. J. Int.*, *155*, 126–138.
- McKenzie, D. (1972), Active tectonics of the Mediterranean regions, *Geophys. J. R. Astron. Soc.*, *30*, 109–185.
- Meghraoui, M., and F. Doumaz (1996), Earthquake-induced folding and paleoseismicity of the El Asnam, fault-related fold, *J. Geophys. Res.*, *101*, 17,617–17,644.

- Meghraoui, M., J. L. Morel, J. Andrieux, and M. Dahmani (1996), Tectonique plio-quadernaire de la chaîne tello-rifaine et de la mer d'Alboran. Une zone complexe de convergence continent-continent, *Bull. Soc. Géol. Fr.*, *167*, 141–157.
- Montenat, C., P. Ott d'Estevou, and P. Masse (1987), Tectonic-sedimentary characters of the Betic Neogene basins evolving in a crustal transcurrent shear zone (SE Spain), *Bull. Cent. Rech. Explor. Prod. Elf-Aquitaine*, *11*, 1–22.
- Morel, J. L., and M. Meghraoui (1996), Gorringe-Alboran-Tell tectonic zone: A transpression system along the Africa-Eurasia plate boundary, *Geology*, *24*, 755–758.
- Pantosti, D., G. D'Addezio, and F. R. Cinti (1996), Paleoseismicity of the Ovindoli-Pezza fault, central Apennines, Italy: A history including a large, previously unrecorded earthquake in Middle Ages (860–1300 A. D.), *J. Geophys. Res.*, *101*, 5937–5959.
- Philip, H., and M. Meghraoui (1983), Structural analysis and interpretation of the surface deformations of the El Asnam earthquake of October 10, 1980, *Tectonics*, *2*, 17–49.
- Platt, J. P., and R. L. M. Vissers (1989), Extensional collapse of thickened continental lithosphere: A working hypothesis for the Alboran Sea and Gibraltar Arc, *Geology*, *17*, 540–543.
- Pondrelli, A. (1999), Patterns of seismic deformation in the Western Mediterranean, *Ann. Geofis.*, *42*, 57–70.
- Reicherter, K. R. (2001), Paleoseismologic advances in the Granada basin (Betic Cordilleras, southern Spain), *Acta Geol. Hispanica*, *36*, 267–281.
- Sanz de Galdeano, C. (1983), Los accidentes y fracturas principales de las Cordilleras Béticas, *Estad. Geol.*, *39*, 157–165.
- Sanz de Galdeano, C. (1990), Geologic evolution of the Betic cordilleras in the western Mediterranean, Miocene to present, *Tectonophysics*, *172*, 107–109.
- Sanz de Galdeano, C., C. López, J. Delgado, and M. A. Peinado (1995), Shallow seismicity and active faults in the Betic Cordillera. A preliminary approach to seismic sources associated with specific faults, *Tectonophysics*, *248*, 293–302.
- Silva, P. G., J. L. Goy, L. Somoza, C. Zazo, and T. Bardají (1993), Landscape response to strike-slip faulting linked to collisional settings: Quaternary tectonics and basin formation in the eastern Betics, southeast Spain, *Tectonophysics*, *224*, 289–303.
- Silva, P. G., J. L. Goy, and C. Zazo (1992), Structural and geometrical features of the Lorca-Alhama strike-slip fault, *Geogaceta*, *12*, 7–11.
- Stich, D., C. J. Ammon, and J. Morales (2003), Moment tensor solutions for small and moderate earthquakes in the Ibero-Maghreb region, *J. Geophys. Res.*, *108*(B3), 2148, doi:10.1029/2002JB002057.
- Swan, F. H. (1988), Temporal clustering of paleoseismic events on the Oued Foda Fault, Algeria, *Geology*, *16*, 1092–1095.
- Udías, A., A. López, and J. Mezcua (1976), Seismotectonic of the Azores-Alboran region, *Tectonophysics*, *31*, 259–289.
- Watts, A. B., J. P. Platt, and P. Buhl (1993), Tectonic evolution of the Alboran Sea basin, *Basin Res.*, *5*, 153–177.
- Wells, D. L., and K. J. Coppersmith (1994), New empirical relationships among magnitude, rupture length, rupture width, rupture area, and surface displacement, *Bull. Seismol. Soc. Am.*, *84*, 974–1002.
- Woodside, J. M., and A. Maldonado (1992), Styles of compressional neotectonics in the eastern Alboran Sea, *Geo Mar. Lett.*, *12*, 111–116.

---

J. L. Hernández-Enrile and J. J. Martínez-Díaz, Departamento de Geodinámica, Facultad de Ciencias Geológicas, Universidad Complutense, Madrid, E-28040 Spain. (jmdiaz@eucmax.sim.ucm.es)

E. Masana and P. Santanach, Departament de Geodinàmica i Geofísica, Universitat de Barcelona, Martí i Franquès s/n, Barcelona, E-08028 Spain. (eula@geo.ub.es; santanac@geo.ub.es)